Computer-based Regressor-free Adaptive Control versus Direct Adaptive Fuzzy Control of the Robotic System

Mahmood Nadali[1], Abolghasem Nadali[2*], Maryam Nadali[3]
[1]Department of Power Electrical, College of Electrical, West Tehran Branch, Islamic Azad University, Tehran, Iran
[2]Department of Computer Engineering, Garmsar Branch, Islamic Azad University, Garmsar, Iran
[3]Master of Industrial Engineering, Signaling Department of Railway, Iran
[*]Email of Corresponding Author: nadali1402@gmail.com
Received:October 24; 2019 Accepted: February 28, 2020

Abstract
A comprehensive comparison between regressor-free control and direct adaptive fuzzy control of flexible-joint robots is addressed in this paper. In the proposed regressor-free controller, two critical practical situations are considered: the fact that robot actuators have limited voltages, and limitation on the number of measurement devices. However, in the article "decentralized direct adaptive fuzzy control for flexible-joint robots," these limitations have been neglected. It should be noted that a few solutions for the voltage-bounded robust tracking control of flexible joint robots have been proposed. In this paper; we contribute to this subject by presenting a new form of voltage-based controllers. The closed-loop control system stability is proved, and uniformly boundedness of the joint position errors is guaranteed. As a second contribution of this paper, we present a robust adaptive control scheme without the need for computation of the regressor matrix with the same result on the closed-loop system stability. Experimental results of the proposed controller and the decentralized direct adaptive fuzzy controller are produced using MATLAB/SIMULINK external mode control on a single-link flexible-joint electrically driven robot. Experimental and analytical results demonstrate the high performance of the proposed control scheme.

Keywords
Actuator Saturation, Direct Adaptive Fuzzy Control, Flexible-joint Robots, Robust Adaptive Control, Voltage Control Strategy

1. Introduction

Flexible joint robots show some considerable advantages in comparison with their rigid counterparts. There are many robotics applications in which soft motions are required. An example of this is surgical robots that high-speed operation and better accuracy are demanded. However, the flexibility of the joints will make the end-effector position control difficult due to unwanted oscillations.

In order to improve the controller performance, i.e., accuracy or suppression of residual vibration, many intelligent and neuro-fuzzy controllers have been proposed [1-6]. In the papers [2-3], neuro-fuzzy controllers based on the assumed mode method have been applied to flexible-joint robots. A supervisory online fuzzy logic controller has been proposed in the research [4]. A neural controller for constrained flexible robots has been presented in [5]. Adaptive neural control of multi-link flexible joint robots in the task-space has been presented in the paper [6]. However, these

approaches [2-6] have excluded the actuator dynamics in their controller design. In other words, the torque applied to the robot joints is the controller outputs in these approaches. Thus, for successful real-time implementation, these controllers should be modified to calculate the voltage applied to electrical motors as the robotic system actuators. Moreover, it should be noted that neglecting the actuator dynamics can lead to inaccuracy in high-speed applications [7]. Thus, voltage-based controllers [1, 8-9] are preferable from a practical point of view.

In [1], a robust control scheme for the flexible-joint electrically driven robot (FJEDR) in the presence of uncertainties associated with both motor and robot dynamics is shown. The proposed approach is related to the critical role of the electrical subsystem of the motors; thus, it is free from a mechanical subsystem of the actuator dynamics, considered here as unmodeled dynamics. As a result, the control design procedure is based on a third-order instead of the fifth-order dynamic model, considering actuator voltage input constraints. An extended form of this work has also been presented [8] that require motor current, motor position, motor velocity, joint position, joint velocity, and joint acceleration for control implementation. The advantage of these approaches is two-loop instead of the three-loop control structure, which makes them superior to others. Nevertheless, their measurement requirements are substantial.

As an extension in the field of electrically flexible joint robots, [9] proposed a single-loop control strategy. Compared with the previous voltage-based control approaches; the proposed control is more uncomplicated. However, it does not consider the saturation nonlinearity in the stability analysis. Furthermore, there exist yet problems arise from Neural network/Fuzzy systems, as mentioned in [10].

In this paper, we are going to extend the results obtained by [9]. First, we improve the stability results of the proposed controller by considering the saturation nonlinearity and external disturbance. The overall closed-loop system composed of full nonlinear robot dynamics for n degrees of freedom and the proposed controller is proved to be stable. At the same time, joint position errors are uniformly bounded. As a second contribution of this paper, we present a robust adaptive control scheme without the need for computation of the regressor matrix. The proposed controller is an alternative to all previous voltage-based control strategies utilized for FJEDR. This novelty gives a simple, robust tracking control scheme for both structured and unstructured uncertainty based on the function approximation technique using the Fourier series expansion [11-13].

This paper is organized as follows. In section 2, the model of an *n*-link flexible joint robot manipulator is described. In Section 3, a direct adaptive fuzzy controller (DAFC) proposed by [9] is reviewed, and its stability analysis is revisited. In section 4, the robust adaptive control scheme is presented. In section 5, some experimental results are provided, and finally, some conclusions are offered in Section 6. Throughout this paper, we use the notation $\underline{\lambda}(\bullet)$ and $\overline{\lambda}(\bullet)$ to indicate the smallest and largest eigen values, respectively, of a positive definite bounded matrix. The norm of vector $\mathbf{y} \in \Re^n$ is defined as $\|\mathbf{y}\| = \sqrt{\mathbf{y}^T \mathbf{y}}$ and that of matrix $\|A(\mathbf{y})\| = \sqrt{\overline{\lambda}\{A(\mathbf{y})^T A(\mathbf{y})\}}$. The vectors and matrices are bold for clarity.

2. Dynamics of Flexible Joint Electrically Driven Robot

The dynamics in the joint space of a serial-chain *n*-link flexible-joint electrically driven robot can be described as

$$\mathbf{D(q)}\ddot{\mathbf{q}} + \mathbf{C(q,\dot{q})}\dot{\mathbf{q}} + \mathbf{g(q)} = \mathbf{K}(\mathbf{r}\boldsymbol{\theta}_m - \mathbf{q}) \quad (1)$$

$$\mathbf{J}\ddot{\boldsymbol{\theta}}_m + \mathbf{B}\dot{\boldsymbol{\theta}}_m + \mathbf{rK}(\mathbf{r}\boldsymbol{\theta}_m - \mathbf{q}) = \mathbf{K}_m\mathbf{I}_a \quad (2)$$

$$\mathbf{RI}_a + \mathbf{L}\dot{\mathbf{I}}_a + \mathbf{K}_b\dot{\boldsymbol{\theta}}_m + \boldsymbol{\varphi}(t) = \mathbf{v}(t) \quad (3)$$

Where $\mathbf{q},\dot{\mathbf{q}},\ddot{\mathbf{q}} \in \Re^n$ are joint position, velocity, and acceleration, respectively, $\mathbf{D(q)} \in \Re^{n\times n}$ is a symmetric, positive-definite function called inertia matrix, $\mathbf{C(q,\dot{q})} \in \Re^{n\times n}$ is a matrix function called centrifugal and Coriolis forces matrix, and $\mathbf{g(q)} \in \Re^n$ is the gravity vector. $\boldsymbol{\theta}_m, \dot{\boldsymbol{\theta}}_m, \ddot{\boldsymbol{\theta}}_m \in \Re^n$ are motor position, velocity, and acceleration, respectively. The constant positive-definite diagonal matrices $\mathbf{K} \in \Re^{n\times n}$, $\mathbf{J} \in \Re^{n\times n}$, $\mathbf{B} \in \Re^{n\times n}$, $\mathbf{r} \in \Re^{n\times n}$, $\mathbf{K}_m \in \Re^{n\times n}$, $\mathbf{L} \in \Re^{n\times n}$, $\mathbf{R} \in \Re^{n\times n}$ and $\mathbf{K}_b \in \Re^{n\times n}$ represent the flexibility, the inertia, the damping constants, the gear-box ratio, the torque constant, the electrical inductance, the electrical resistance, and the back-emf effects of the actuators, respectively. $\mathbf{I}_a \in \Re^n$ Is the armature current vector $\boldsymbol{\varphi}(t) \in \Re^n$ Represents the external disturbance and $\mathbf{v}(t) \in \Re^n$ denotes the control input voltage applied for the joint actuators.

3. Revisiting Considering Actuator Voltage input Constraint [9]

The presented model given by Equations (1) to (3) is a fifth-order nonlinear and dynamically coupled multivariable system that makes the control problem extremely difficult. To tackle this problem, a decentralized robust tracking controller has been developed in [9] by employing voltage as a control input signal. Let us define:

$$(\mathbf{r}\boldsymbol{\theta}_m - \mathbf{q}) = \boldsymbol{\delta} \quad (4)$$

Where $\boldsymbol{\delta}$ represents the effect of joint flexibility. Combining Equations (2) and (4) gives

$$\mathbf{J}\ddot{\boldsymbol{\theta}}_m + \mathbf{B}\dot{\boldsymbol{\theta}}_m + \mathbf{rK}\boldsymbol{\delta} = \mathbf{K}_m\mathbf{I}_a \quad (5)$$

Using Equations (3), (4) and (5), a decoupled dynamic equation can then be written as [9]:

$$\ddot{\mathbf{q}} + \mathbf{K}_a\dot{\mathbf{q}} + \boldsymbol{\mu} = \mathbf{K}_v\,\mathbf{v}(t) \quad (6)$$

Where

$$\mathbf{K}_a = \mathbf{J}^{-1}(\mathbf{B} + \mathbf{K}_m\mathbf{R}^{-1}\mathbf{K}_b) \quad (7)$$

$$\mathbf{K}_v = \mathbf{rJ}^{-1}\mathbf{K}_m\mathbf{R}^{-1} \quad (8)$$

And

$$\boldsymbol{\mu} = \ddot{\boldsymbol{\delta}} + \mathbf{K}_a\dot{\boldsymbol{\delta}} + \mathbf{J}^{-1}\mathbf{r}^2\mathbf{K}\boldsymbol{\delta} + \mathbf{K}_v(\mathbf{L}\dot{\mathbf{I}}_a + \boldsymbol{\varphi}(t)) \quad (9)$$

In order to design a decentralized controller, assume that the dynamics of the ith joint can be represented by

$$\ddot{q} + K_a\dot{q} + \mu = K_v\,\mathrm{v}(t)$$

Where the presented variables $\dot{q}, \ddot{q}$, μ, and $\mathrm{v}(t)$ are the ith element of the vector $\dot{\mathbf{q}}, \ddot{\mathbf{q}}, \boldsymbol{\mu}$ and $\mathbf{v}(t)$, respectively. The coefficients K_a and K_v are also the ith element of the diagonal matrices $\mathbf{K}_a$ and

$\mathbf{K}_v$, respectively.

For a practical situation, the actuator inputs are subjected to some constraints, called motor saturation limits. It occurs usually between the output of the controller and the PWM module [14]. For the development in this paper, we assume that the relation between the actual actuator input $\mathrm{v}(t)$ and control signal produced by the controller $\mathrm{u}(t)$ is given by

$$\mathrm{v}(t)=\mathrm{sat}(\mathrm{u}(t)) \tag{10}$$

Where $\mathrm{sat}(\mathrm{u}(t)) \in \Re$ is the saturation function. According to [14], the hard saturation function can be divided into a linear function $\mathrm{u}(t)$ and a dead-zone function $\mathrm{dzn}(\mathrm{u}(t), u_{\max})$. Thus, the control input applied to the system through the actuator is expressed as follows:

$$\mathrm{sat}(\mathrm{u}(t))=\mathrm{u}(t)-\mathrm{dzn}(\mathrm{u}(t), u_{\max}) \tag{11}$$

Now, substituting Equations (11) into (10), and using Equation (6), it follows that

$$\ddot{q}+K_a\dot{q}+\mu=K_v\,\mathrm{u}(t)-K_v\,\mathrm{dzn}(\mathrm{u}(t), u_{\max}) \tag{12}$$

Remark 1**:** The control input given by Equation (10) indicates that the motor voltage is bounded, that is

$$\left|\mathrm{v}(t)\right| \le \mathrm{u}_{\max} \tag{13}$$

Where $\mathrm{u}_{\max}$ is a positive constant representing the maximum permitted voltage of the motor [14]. As a result, the variables I_a, $\dot{I}_a$ and $\dot{\theta}_m$ are upper bounded by ξ_I , $\xi_{\dot{I}}$ and $\xi_{\dot{\theta}_m}$, respectively.

Following the same procedure, as described in [9], using Mamani type inference-engine, singleton-fuzzifier and center-average defuzzifier, we propose a fuzzy controller in the form of

$$\mathrm{u}(t)=\hat{\mathbf{y}}^{\mathrm{T}}\boldsymbol{\psi}(x_1, x_2) \tag{14}$$

Where $\hat{\mathbf{y}}$ is the estimation of $\mathbf{y}$ used into the fuzzy system $\mathbf{y}^{\mathrm{T}}\boldsymbol{\psi}(x_1, x_2)$ which approximates the following function based on the universal approximation theorem of fuzzy systems as

$$\mathbf{y}^{\mathrm{T}}\boldsymbol{\psi}(x)+\varepsilon=K_v^{-1}(\ddot{q}_d+k_1\dot{e}+k_d x_2+k_p x_1+K_a\dot{q}+\mu) \tag{15}$$

Where $\boldsymbol{\psi}(x) \in \Re^N$ denotes fuzzy basis function vector fixed by the designer, the number N represents the number of fuzzy linguistic rules, ε is reconstruction error of fuzzy logic system; q_d is the desired joint position, k_1, k_d and k_p are positive scalar gains which are selected as control design parameters,

$$x_1=e+k_1\int_0^t e(\tau)d\tau \tag{16}$$

$$x_2=\dot{e}+k_1 e \tag{17}$$

And e is tracking error expressed by

$$e=q_d-q \tag{18}$$

In order to obtain the adaptive control law, we form the tracking system from Equations (15), (16), and (18) as

$$\dot{x}_2+k_d x_2+k_p x_1=K_v\tilde{\mathbf{y}}^{\mathrm{T}}\boldsymbol{\psi}+K_v\varepsilon+K_v\,\mathrm{dzn}(\mathrm{u}(t), u_{\max}) \tag{19}$$

Where $\tilde{\mathbf{y}} = \mathbf{y} - \hat{\mathbf{y}}$ The state-space equation in the tracking space is then obtained using Equation (19) as

$$\dot{\mathbf{X}} = \mathbf{A}\mathbf{X} + \mathbf{B}(K_v \tilde{\mathbf{y}}^{\mathrm{T}} \boldsymbol{\psi} + K_v \varepsilon + K_v \,\mathrm{dzn}(\mathrm{u}(t), u_{\max})) \tag{20}$$

Where

$$\mathbf{A} = \begin{bmatrix} 0 & 1 \\ -k_p & -k_d \end{bmatrix}, \quad \mathbf{B} = \begin{bmatrix} 0 \\ 1 \end{bmatrix}, \quad \mathbf{X} = \begin{bmatrix} x_1 \\ x_2 \end{bmatrix} \tag{21}$$

3.1 Stability Analysis

Before starting the stability analysis, the following lemma is given. First, we present the following three assumptions, which are required in determining the sufficient conditions on the control parameters.

Assumption 1: The desired trajectory and its time derivative are in L_∞ space $(q_d, \dot{q}_d \in L_\infty)$.

Assumption 2: The external disturbance $\phi(t)$ is bounded as

$$|\varphi(t)| \le \varphi_{\max} \tag{22}$$

Where $\varphi_{\max}$ is a positive constant.

Assumption 3: The reconstruction error ε is bounded, i.e. $|\varepsilon| < \varepsilon_c$ with known ε_c.

Now, we are ready to present the following lemma.

Lemma 1. $|\mathrm{dzn}(\mathrm{u}(t))|$ is satisfied with the following condition:

$$|\mathrm{dzn}(\mathrm{u}(t), u_{\max})| \le \frac{\delta u_{\max}}{(1-\delta)} \tag{23}$$

Where δ is a constant, which always has a value smaller than 1.

Proof : Suppose that $\mathrm{u}(t)$ exists in the interval $[-\max\{\mathrm{u}(t)\}, \max\{\mathrm{u}(t)\}]$ and δ is $\max\left\{1 - \frac{u_{\max}}{\mathrm{u}(t)}\right\}$.

Then,

$$|\mathrm{dzn}(\mathrm{u}(t), u_{\max})| \le \delta |\mathrm{u}(t)| \tag{24}$$

It is satisfied by Figure 1.

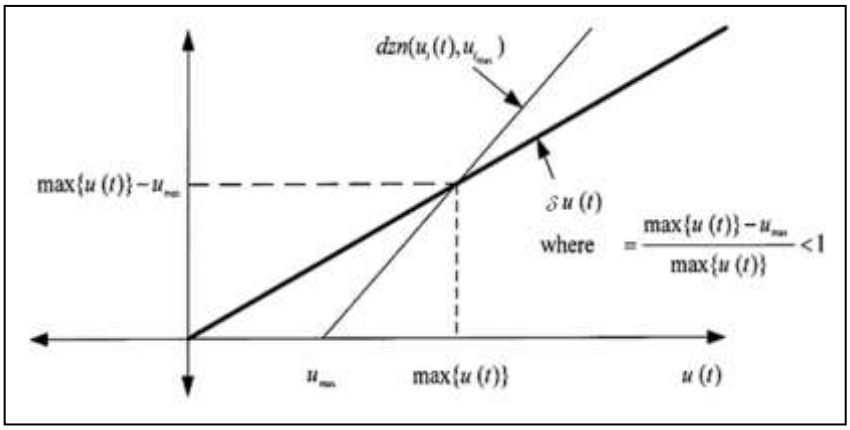

Figure1. Linear bound of dead-zone function

This result, together with Equations (14), (15) and (24) gives

$$\begin{aligned}\left|\mathrm{dzn}(\mathrm{u}(t),u_{\max})\right| &\le \delta\left|\mathbf{y}^{\mathrm{T}}\boldsymbol{\psi}+\varepsilon-K_v^{-1}\left(\dot{x}_2+k_d x_2+k_p x_1\right)+\mathrm{dzn}(\mathrm{u}(t),u_{\max})\right| \\ &\le \delta\left|K_v^{-1}\left(\ddot{q}+K_a\dot{q}+\mu\right)\right|+\delta\left|\mathrm{dzn}(\mathrm{u}(t),u_{\max})\right|\end{aligned} \tag{25}$$

Now, according to (14), (15), and (25), we have:

$$\left|\mathrm{dzn}(\mathrm{u}(t),u_{\max})\right| \le \frac{\delta u_{\max}}{(1-\delta)}$$

It completes the proof■

Now, to carry out the stability analysis of the closed-loop system formed by dynamic Equation (10), the following positive definite function is proposed:

$$V(\mathbf{X},\tilde{\mathbf{y}}) = \frac{1}{2}\mathbf{X}^T\mathbf{P}\mathbf{X}+\frac{K_v}{2\alpha}\tilde{\mathbf{y}}^T\tilde{\mathbf{y}} \tag{26}$$

Where the constant $\alpha>0$, $\mathbf{P}$ and $\mathbf{Q}$ are the unique symmetric, positive definite matrices satisfying the matrix Lyapunov equation

$$\mathbf{A}^T\mathbf{P}+\mathbf{P}\mathbf{A}=-\mathbf{Q} \tag{27}$$

By differentiating (26) along the trajectories of the uncertain system (19) and rearranging with some manipulation, it leads to

$$\begin{aligned}\dot{V}(\mathbf{X},\tilde{\mathbf{y}}) = &-\frac{1}{2}\mathbf{X}^T\mathbf{Q}\mathbf{X}+\mathbf{X}^T\mathbf{P}\mathbf{B}K_v\varepsilon+\mathbf{X}^T\mathbf{P}\mathbf{B}K_v\,\mathrm{dzn}(\mathrm{u}(t),u_{\max}) \\ &+K_v\tilde{\mathbf{y}}^T\boldsymbol{\psi}\mathbf{B}^T\mathbf{P}\mathbf{X}-\frac{K_v}{\alpha}\tilde{\mathbf{y}}^T\dot{\hat{\mathbf{y}}}\end{aligned} \tag{28}$$

If the update law is given by

$$\dot{\hat{\mathbf{y}}} = \alpha\boldsymbol{\psi}\mathbf{B}^T\mathbf{P}\mathbf{X} \tag{29}$$

Then, we have

$$\dot{V}(\mathbf{X},\tilde{\mathbf{y}}) \le -\frac{1}{2}\underline{\lambda}(\mathbf{Q})\|\mathbf{X}\|^2+\|\mathbf{P}_2\|K_v\|\mathbf{X}\|\left(|\varepsilon|+\left|\mathrm{dzn}(\mathrm{u}(t),u_{\max})\right|\right) \tag{30}$$

Where $\mathbf{P}_2$ is the second column of $\mathbf{P}$. Now, according to Lemma 1 and assumption 3 we have

$$\dot{V}(\mathbf{X},\tilde{\mathbf{y}}) \le -\frac{1}{2}\underline{\lambda}(\mathbf{Q})\|\mathbf{X}\|^2+\|\mathbf{P}_2\|K_v\|\mathbf{X}\|\left(\varepsilon_c+\frac{\delta u_{\max}}{(1-\delta)}\right) \tag{31}$$

Therefore, $\dot{V}(\mathbf{X},\tilde{\mathbf{y}})$ is negative definite as long as $\|\mathbf{X}\|$ is outside the compact set $\Omega_{\mathbf{X}}$ defined as

$$\Omega_{\mathbf{X}} = \left\{\mathbf{X}\middle|\|\mathbf{X}\| \le \beta = \frac{2\|\mathbf{P}_2\|K_v}{\underline{\lambda}(\mathbf{Q})}\left(\varepsilon_c+\frac{\delta u_{\max}}{(1-\delta)}\right)\right\} \tag{32}$$

It means that $\mathbf{X}$ and $\tilde{\mathbf{y}}$ are bounded. According to the definition of x_1, and x_2, the linear equation $\dot{e}+k_1e=x_2$ has the bounded input x_2, thereby e and $\dot{e}$ are bounded. Since $e=q_d-q$ and $\dot{e}=\dot{q}_d-\dot{q}$, thus boundedness of e, and $\dot{e}$ follows boundedness of q, and $\dot{q}$ according to assumption 1. Extending this result to all motors implies the boundedness of system states $\mathbf{q}$ and $\dot{\mathbf{q}}$. From Equation (2) we have

$$\mathbf{J}\ddot{\boldsymbol{\theta}}_m + \mathbf{B}\dot{\boldsymbol{\theta}}_m + \mathbf{r}^2\mathbf{K}\boldsymbol{\theta}_m = \mathbf{K}_m\mathbf{I}_a + \mathbf{rq} \tag{33}$$

Since $\mathbf{J}$, $\mathbf{B}$ and $\mathbf{r}^2\mathbf{K}$ are positive diagonal matrices, the second-order linear system expressed by Equation (33) is stable with the bounded input $\mathbf{K}_m\mathbf{I}_a + \mathbf{rq}$, according to remark 1. As a result, the output is bounded. In summary, all system states are bounded. Thus, it is concluded that the proposed DAFC has guaranteed stability.

Remark 2: The radius of the compact set $\Omega_{\mathbf{X}}$ is related to the other parameters except for approximation error.

4. The Robust Adaptive Control Scheme

The presented approach given by [9] is straightforward. However, there exist yet problems originated from Neural Network/Fuzzy systems, as mentioned in [10]. As a second contribution, in this paper, a FAT-based robust control strategy is developed that eliminates the problem above. Toward this end, assume that Equation (12) for the i-th joint can be reformulated as

$$\ddot{q} + \wp(t) = \mathrm{u}(t) \tag{34}$$

Where $\wp(t)$ is called residual uncertainty denoted by

$$\wp(t) = K_a\dot{q} + \mu + K_v\,\mathrm{dzn}(\mathrm{u}(t), u_{\max}) + (1 - K_v)\mathrm{u}(t) \tag{35}$$

Remark 3: According to [9], the uncertain function which should be estimated can include the control signal $\mathrm{u}(t)$.

Before we go to the details of controller derivation, we present the following assumption.

Assumption 4. A nonlinear function $\wp(t)$ is assumed to be an unknown bounded function, and its variation bound is also assumed to be unavailable.

As a result of Assumption 4, the traditional adaptive control scheme is not applicable. Under these circumstances, a simple control law is proposed as

$$\mathrm{u}(t) = \ddot{q}_d + \Gamma_d(\dot{q}_d - \dot{q}) + \Gamma_p(q_d - q) + \hat{\wp}(t) \tag{36}$$

Where Γ_p and Γ_d are positive proportional and derivative scalar gains, respectively, and $\hat{\wp}(t)$ is the estimate of $\wp(t)$. Substituting (36) into (34) gives

$$\ddot{e} + \Gamma_d\dot{e} + \Gamma_p e = \wp(t) - \hat{\wp}(t) \tag{37}$$

Where e is the same as before. Define $\boldsymbol{\Lambda}$ and $\mathbf{H}$ as

$$\boldsymbol{\Lambda} = \begin{bmatrix} 0 & 1 \\ -\Gamma_p & -\Gamma_d \end{bmatrix}, \quad \mathbf{H} = \begin{bmatrix} 0 \\ 1 \end{bmatrix} \tag{38}$$

The error equation (37) can then be written in the following state-space form

$$\dot{\mathbf{x}} = \boldsymbol{\Lambda}\mathbf{x} + \mathbf{H}(\wp(t) - \hat{\wp}(t)) \tag{39}$$

Where $\mathbf{x} = [e \quad \dot{e}]^T \in \Re^2$ is the state vector. If an appropriate update law for $\hat{\wp}(t)$ can be designed,

so that $\hat{\wp}(t) \to \wp(t)$; then Equation (37) can give the desired performance. With this in mind, the function approximation technique will be used to represent $\wp(t)$ as linear combinations of basic functions as

$$\wp(t) = \mathbf{W}_{\wp}^T \mathbf{Z}_{\wp} + \varepsilon_{\wp} \tag{40}$$

Where $\mathbf{W}_{\wp} \in \Re^{\Upsilon}$ is weighting vector, Υ is the number of basis functions used, $\mathbf{Z}_{\wp} \in \Re^{\Upsilon}$ is the vector of basis functions and $\varepsilon_{\wp}$ is the approximation error of $\wp(t)$. Making use the same set of basis functions, we propose

$$\hat{\wp}(t) = \hat{\mathbf{W}}_{\wp}^T \mathbf{Z}_{\wp} \tag{41}$$

Where $\hat{\mathbf{W}}_{\wp} \in \Re^{\Upsilon}$ is the estimation of $\mathbf{W}_{\wp}$. Now, substituting Equations (40) and (41) into (39) yields the closed-loop error dynamic as

$$\dot{\mathbf{x}}(t) = \mathbf{\Lambda}\mathbf{x}(t) + \mathbf{H}\tilde{\mathbf{W}}_{\wp}^T \mathbf{Z}_{\wp} + \mathbf{H}\varepsilon_{\wp} \tag{42}$$

Where $\tilde{\mathbf{W}}_{\wp} = \mathbf{W}_{\wp} - \hat{\mathbf{W}}_{\wp}$ is the Fourier-series weights approximation error. Then, our main results can be formulated as the following theorem.

Theorem 1: Given the system in Equation (42) and Assumptions 4, choose the FAT-based tracking control laws (37) and (39) with the Υ number of basis functions for uncertainty approximation. Let the tuning laws with σ-modification for the estimated vectors $\hat{\mathbf{W}}_{\wp}$ be as

$$\dot{\hat{\mathbf{W}}}_{\wp} = \mathbf{Q}_{\wp}^{-1}(\mathbf{Z}_{\wp}\mathbf{H}^T\mathbf{P}\mathbf{x} - \sigma_{\wp}\hat{\mathbf{W}}_{\wp}) \tag{43}$$

Where $\mathbf{Q}_{\wp} \in \Re^{\Upsilon \times \Upsilon}$ is a positive definite constant matrix and $\sigma_{\wp}$ is a positive number. By properly selecting the control gains, design parameters, and the sufficient number of basis functions, the tracking error $\mathbf{x}(t)$ and the weighting vector $\tilde{\mathbf{W}}_{\wp}$ are uniformly ultimately bounded.

Proof: Consider a positive definite function as

$$V(\mathbf{x}, \tilde{\mathbf{W}}_{\wp}) = \mathbf{x}^T\mathbf{P}\mathbf{x} + \tilde{\mathbf{W}}_{\wp}^T\mathbf{Q}_{\wp}\tilde{\mathbf{W}}_{\wp} \tag{44}$$

Differentiating Equation (43) concerning time, using (41) and (42), it can obtain that

$$\dot{V}(\mathbf{x}, \tilde{\mathbf{W}}_{\wp}) = \mathbf{x}^T(\mathbf{\Lambda}^T\mathbf{P} + \mathbf{P}\mathbf{\Lambda})\mathbf{x} + 2\mathbf{x}^T\mathbf{P}\mathbf{H}\varepsilon_{\wp} + 2\sigma_{\wp}\tilde{\mathbf{W}}_{\wp}^T\hat{\mathbf{W}}_{\wp} \tag{45}$$

Since $\mathbf{\Lambda}$ is Hurwitz, one can arbitrarily choose a positive definite matrix $\mathbf{Q}$ and let $\mathbf{P}$ be the unique symmetric positive-definite matrix that satisfies the Lyapunov equation

$$\mathbf{\Lambda}^T\mathbf{P} + \mathbf{P}\mathbf{\Lambda} = -\mathbf{Q} \tag{46}$$

Equation (45) can be, therefore, rewritten as

$$\begin{aligned}\dot{V}(\mathbf{x}, \tilde{\mathbf{W}}_{\wp}) &= -\mathbf{x}^T\mathbf{Q}\mathbf{x} + 2\mathbf{x}^T\mathbf{P}\mathbf{H}\varepsilon_{\wp} + 2\sigma_{\wp}\tilde{\mathbf{W}}_{\wp}^T\hat{\mathbf{W}}_{\wp} \\ &\le -\lambda_{\min}(\mathbf{Q})\|\mathbf{x}\|^2 + 2\lambda_{\max}(\mathbf{P})|\varepsilon_{\wp}|\|\mathbf{x}\| + 2\sigma_{\wp}\left(\tilde{\mathbf{W}}_{\wp}^T\mathbf{W}_{\wp} - \|\tilde{\mathbf{W}}_{\wp}\|^2\right)\end{aligned} \tag{47}$$

Result 1: Suppose a sufficient number of basis functions are used, and the approximation error can be ignored, then it is not necessary to include the σ-modification terms in Equation (45). Hence, Equation (47) can be reduced to

$$\dot{V}(\mathbf{x},\tilde{\mathbf{W}}_{\wp}) \le -\lambda_{\min}(\mathbf{Q})\|\mathbf{x}\|^2 \le 0 \tag{48}$$

And asymptotic convergence of $\mathbf{x}$ can be concluded using the Barbalat's Lemma.

Result 2: Owing to the existence of $\varepsilon_{\wp}$ in Equation (47), it may be assumed the negative definiteness of $\dot{V}$ be guaranteed. In the following, we would like to investigate the system stability in the presence of reconstruction errors. It is effortless to prove the inequalities hold

$$\begin{aligned} -\lambda_{\min}(\mathbf{Q})\|\mathbf{x}\|^2 + 2\lambda_{\max}(\mathbf{P})|\varepsilon_{\wp}|\|\mathbf{x}\| &\le -\frac{1}{2}\lambda_{\min}(\mathbf{Q})\|\mathbf{x}\|^2 + \frac{2\lambda_{\max}^2(\mathbf{P})}{\lambda_{\min}(\mathbf{Q})}\varepsilon_{\wp}^2, \\ \tilde{\mathbf{W}}_{\wp}^T\mathbf{W}_{\wp} - \|\tilde{\mathbf{W}}_{\wp}\|^2 &\le \frac{1}{2}(\|\mathbf{W}_{\wp}\|^2 - \|\tilde{\mathbf{W}}_{\wp}\|^2) \end{aligned} \tag{49}$$

Using Equation (48), we obtain

$$\dot{V}(\mathbf{x},\tilde{\mathbf{W}}_{\wp}) \le -\frac{1}{2}\lambda_{\min}(\mathbf{Q})\|\mathbf{x}\|^2 - \sigma_{\wp}\|\tilde{\mathbf{W}}_{\wp}\|^2 + \frac{2\lambda_{\max}^2(\mathbf{P})}{\lambda_{\min}(\mathbf{Q})}\varepsilon_{\wp}^2 + \sigma_{\wp}\|\mathbf{W}_{\wp}\|^2 \tag{50}$$

Note that

$$V(\mathbf{x},\tilde{\mathbf{W}}_{\wp}) \le \lambda_{\max}(\mathbf{P})\|\mathbf{x}\|^2 + \lambda_{\max}(\mathbf{Q}_{\wp})\|\tilde{\mathbf{W}}_{\wp}\|^2 \tag{51}$$

Then, Equation (51) can be further derived as

$$\begin{aligned} \dot{V}(\mathbf{x},\tilde{\mathbf{W}}_{\wp}) \le -\mu N &+ (\mu\lambda_{\max}(\mathbf{P}) - \frac{1}{2}\lambda_{\min}(\mathbf{Q}))\|\mathbf{x}\|^2 \\ &+ (\mu\lambda_{\max}(\mathbf{Q}_{\wp}) - \sigma_{\wp})\|\tilde{\mathbf{W}}_{\wp}\|^2 + \frac{2\lambda_{\max}^2(\mathbf{P})}{\lambda_{\min}(\mathbf{Q})}\varepsilon_{\wp}^2 + \sigma_{\wp}\|\mathbf{W}_{\wp}\|^2 \end{aligned} \tag{52}$$

Picking $\mu \le \min\left\{\frac{\lambda_{\min}(\mathbf{Q})}{2\lambda_{\max}(\mathbf{P})}, \frac{\sigma_{\wp}}{\lambda_{\max}(\mathbf{Q}_{\wp})}\right\}$, the second and third terms of Equation (52) becomes negative, and thus

$$\dot{V}(\mathbf{x},\tilde{\mathbf{W}}_{\wp}) \le -\mu N + \frac{2\lambda_{\max}^2(\mathbf{P})}{\lambda_{\min}(\mathbf{Q})}\varepsilon_{\wp}^2 + \sigma_{\wp}\|\mathbf{W}_{\wp}\|^2 \tag{53}$$

The last Equation is guaranteed to be negative as long as

$$V > \frac{2\lambda_{\max}^2(\mathbf{P})}{\mu\lambda_{\min}(\mathbf{Q})}\sup_{t_0<\tau<t}\varepsilon_{\wp}^2(\tau) + \frac{\sigma_{\wp}}{\mu}\|\mathbf{W}_{\wp}\|^2 \tag{54}$$

Hence, we have proved that $(\mathbf{x},\tilde{\mathbf{W}}_{\wp})$ is uniformly, ultimately bounded.■

4.1 Performance Evaluation

The above derivation only demonstrates the boundedness of $(\mathbf{x},\tilde{\mathbf{W}}_{\wp})$, but in practical applications, the transient performance is also of great importance. For further development, we may solve the differential inequality in Equation (51) to have the upper bound for $V(\mathbf{x},\tilde{\mathbf{W}}_{\wp})$.

$$V(\mathbf{x},\tilde{\mathbf{W}}_{\wp}) \le e^{-\mu(t-t_0)}V(t_0) + \frac{2\lambda_{\max}^2(\mathbf{P})}{\mu\lambda_{\min}(\mathbf{Q})}\sup_{t_0<\tau<t}\varepsilon_{\wp}^2(\tau) + \frac{\sigma_{\wp}}{\mu}\|\mathbf{W}_{\wp}\|^2 \tag{55}$$

Using the inequality

$$V(\mathbf{x},\tilde{\mathbf{W}}_{\wp}) \geq \lambda_{\min}(\mathbf{P})\|\mathbf{x}\|^2 + \lambda_{\min}(\mathbf{Q}_{\wp})\left\|\tilde{\mathbf{W}}_{\wp}\right\|^2 \tag{56}$$

We may find the upper bound for $\|\mathbf{x}\|$ as

$$\|\mathbf{x}\| \leq \sqrt{\frac{V(t_0)}{\lambda_{\min}(\mathbf{P})}}e^{\frac{-\mu(t-t_0)}{2}} + \sqrt{\frac{2\lambda_{\max}^2(\mathbf{P})}{\mu\lambda_{\min}(\mathbf{P})\lambda_{\min}(\mathbf{Q})}}\sup_{t_0<\tau<t}\left|\varepsilon_{\wp}(\tau)\right| + \sqrt{\frac{\sigma_{\wp}}{\mu\lambda_{\min}(\mathbf{P})}}\left\|\mathbf{W}_{\wp}\right\| \tag{57}$$

It implies that the magnitude of the $\|\mathbf{x}\|$ is bounded by an exponential function plus some constants. It also implies that by adjusting controller parameters, we may improve the output error convergence rate. As a consequence,

$$\lim_{t\to\infty}\|\mathbf{x}\| \leq \sqrt{\frac{2\lambda_{\max}^2(\mathbf{P})}{\mu\lambda_{\min}(\mathbf{P})\lambda_{\min}(\mathbf{Q})}}\sup_{t_0<\tau<t}\left|\varepsilon_{\wp}(\tau)\right| + \sqrt{\frac{\sigma_{\wp}}{\mu\lambda_{\min}(\mathbf{P})}}\left\|\mathbf{W}_{\wp}\right\| \tag{58}$$

With the same procedure as done for $\|\mathbf{x}\|$, we can find the following upper bound for the weighting vector $\tilde{\mathbf{W}}_{\wp}$.

$$\lim_{t\to\infty}\left\|\tilde{\mathbf{W}}_{\wp}\right\| \leq \sqrt{\frac{2\lambda_{\max}^2(\mathbf{P})}{\mu\lambda_{\min}(\mathbf{Q}_{\wp})\lambda_{\min}(\mathbf{Q})}}\sup_{t_0<\tau<t}\left|\varepsilon_{\wp}(\tau)\right| + \sqrt{\frac{\sigma_{\wp}}{\mu\lambda_{\min}(\mathbf{Q}_{\wp})}}\left\|\mathbf{W}_{\wp}\right\| \tag{59}$$

The transient performance analysis is then completed.■

5. Experimental Results

The laboratory set up which has been considered for the experimental study is shown in Figure 2.

Figure2. Experimental setup

It is a single-link flexible joint manipulator. The joint consists of two aluminum plates joined by polyurethane material to possess high flexibility. The actuator is a geared permanent magnet DC motor, operating within ±12 volt input, directly driving one plate. A steel tube is connected to the

second plate. Two potentiometers provide feedback of the motor and joint positions, while velocity information is obtained by filtering the position feedback data [15]. In order to control the system using a PC, a PCL-818 I/O card and a PCLD-8115D data acquisition card of the Advantech Company are used for hardware interfacing. The "Real-Time Workshop" facilities of the MATLAB SIMULINK are used for the user interface. A block diagram of the system is shown in Figure 3.

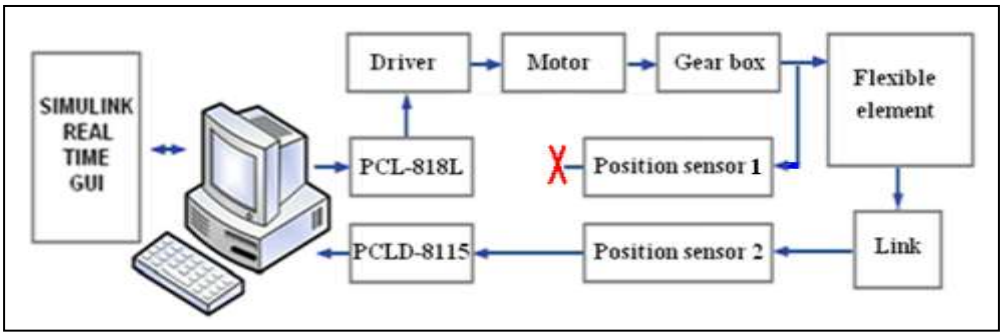

Figure3. Block diagram of the system

To explore the controllers' ability, the performance of the proposed control methods (Equations (39), (43) and (45)) is compared with direct adaptive fuzzy control given by [9]. The desired trajectory $q_d(t)$ used in all experiments is given by

$$q_d(t) = 1.26 - 0.63\sin(\frac{2\pi}{5}t) \tag{60}$$

The following gains are used for each controller.

1) For DAFC given by [9], $\sigma = 0.5$, and $\alpha = 2$. Three membership functions are given to the fuzzy variables q and $\dot{q}$ in the operating range of the system. Thus, the whole space is covered by 9 fuzzy rules. The membership functions are chosen the same as [9], and the fuzzy linguistic rules are proposed in the form of Mamdani, as mentioned in [9].

2) The proposed approach: $\Gamma_p = 150$, $\Gamma_d = 24.45$. The five first terms of Fourier series as the basis functions for the approximation are used in (40). Therefore, $\hat{\mathbf{W}}_{\wp}$ is in $\Re^5$. The initial weighting vector for the entries is assigned to zero, and the gain matrix in the update law (42) is selected as $\mathbf{Q}_{\wp} = 50I_5$, where $I_{(.)}$ is the identity matrix.

Under these settings, experimental results in the absence of external disturbance were presented in Figures 4-7. Figure 4 shows the desired and actual joint angular positions.

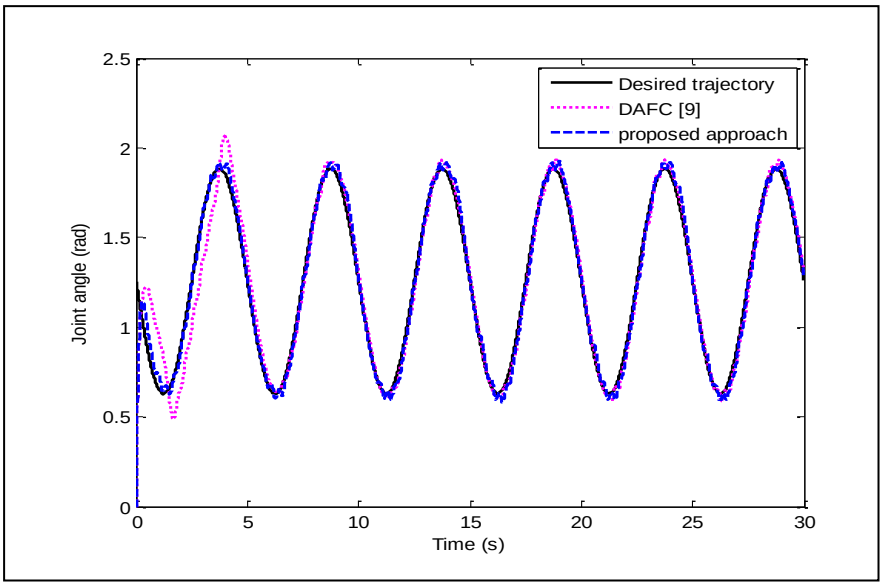

Figure4. Output tracking performance

Joint position errors are shown in Figure 5.

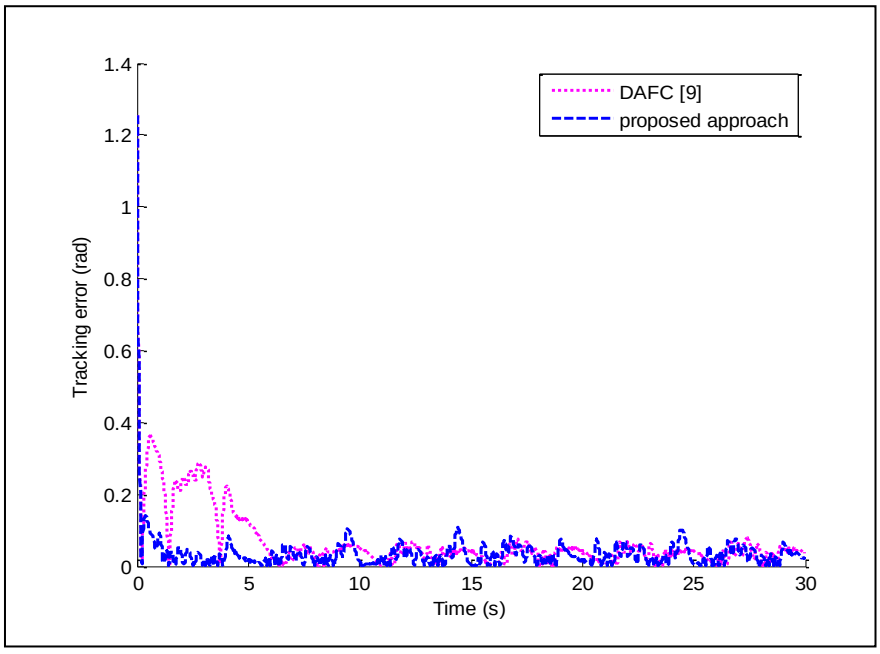

Figure5. Joint position errors

The applied voltages are shown in Figure 6.

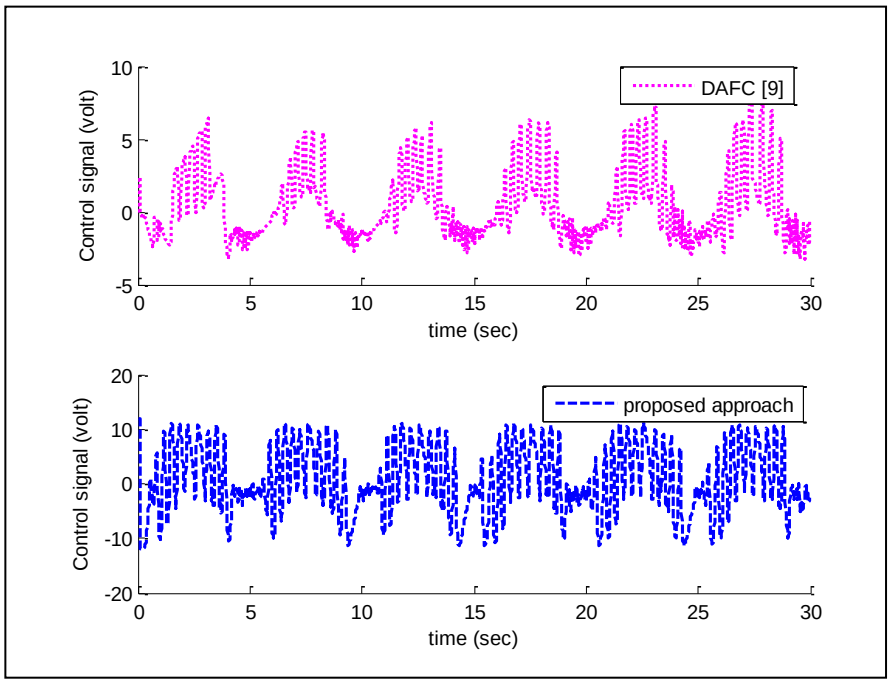

Figure6. Control signal

Finally, Figure 7 shows the time evolution of the approximation of $\hat{\wp}(t)$.

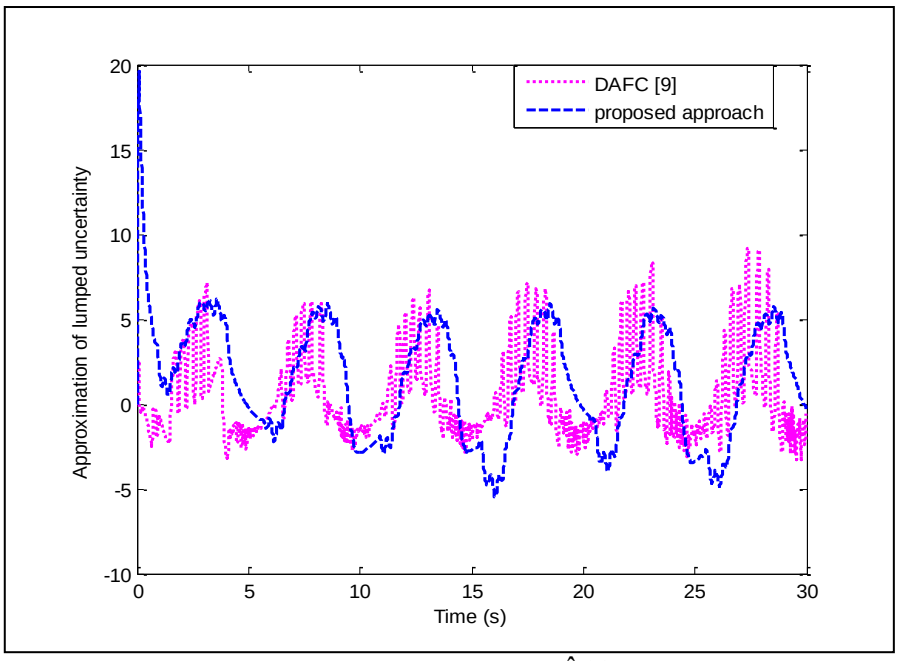

Figure7. Approximation of $\hat{\wp}(t)$

As can be seen, all controllers approximately have the same result in the tracking of the desired trajectory in the absence of external disturbances.

To test the performance robustness of the controllers to external disturbances, a unit step disturbance with amplitude 60 volt is added to the system at t=15sec. The results of the

implementation of DAFC [9], and the proposed control scheme, are illustrated in Figures 8-11, which show the output tracking performance, the absolute value of joint position error, the time evolution of the applied voltage, and approximation of $\hat{\wp}(t)$, respectively. As can be seen, more accuracy is obtained with the proposed control scheme.

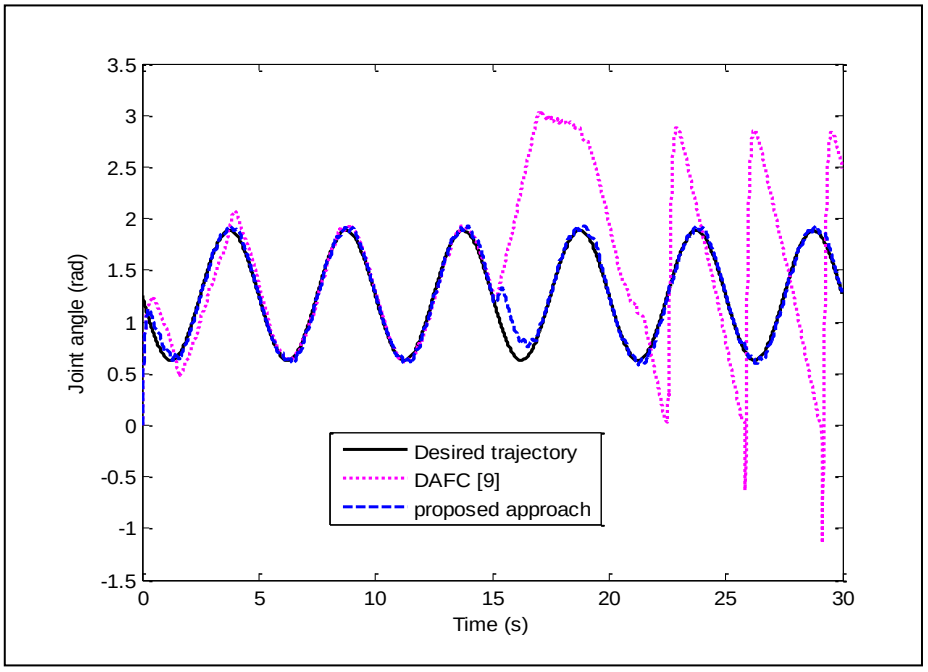

Figure8. Output tracking performance

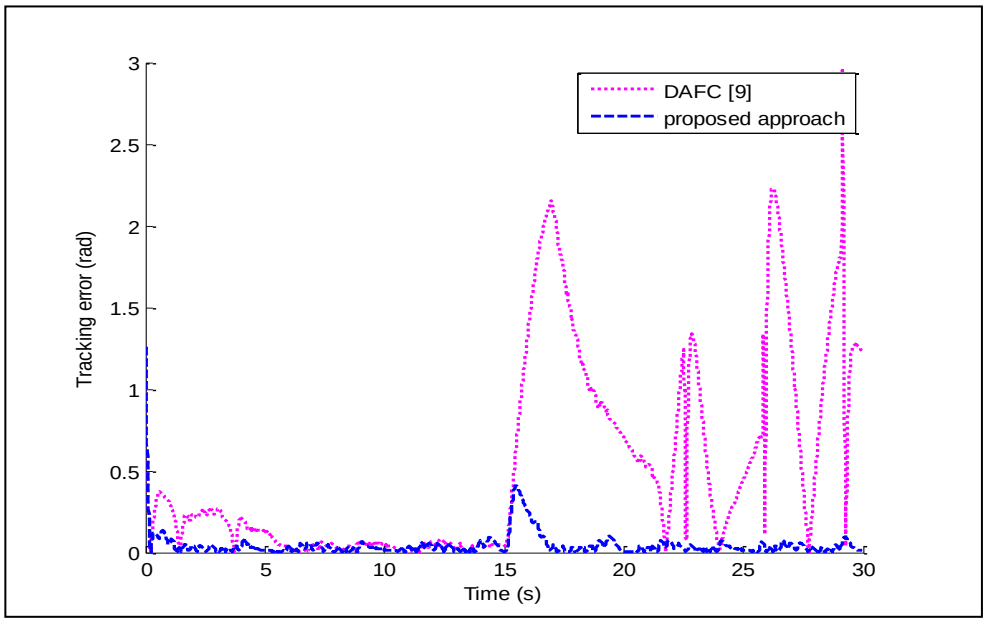

Figure9. Joint position errors

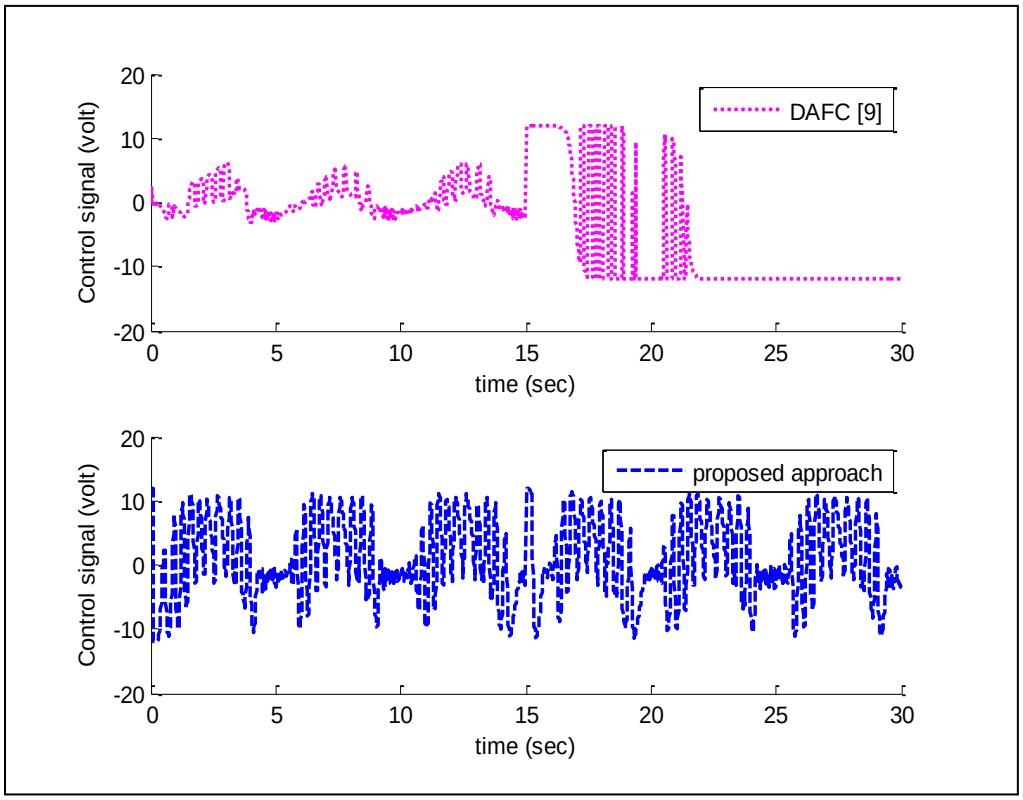

Figure10. Control signal

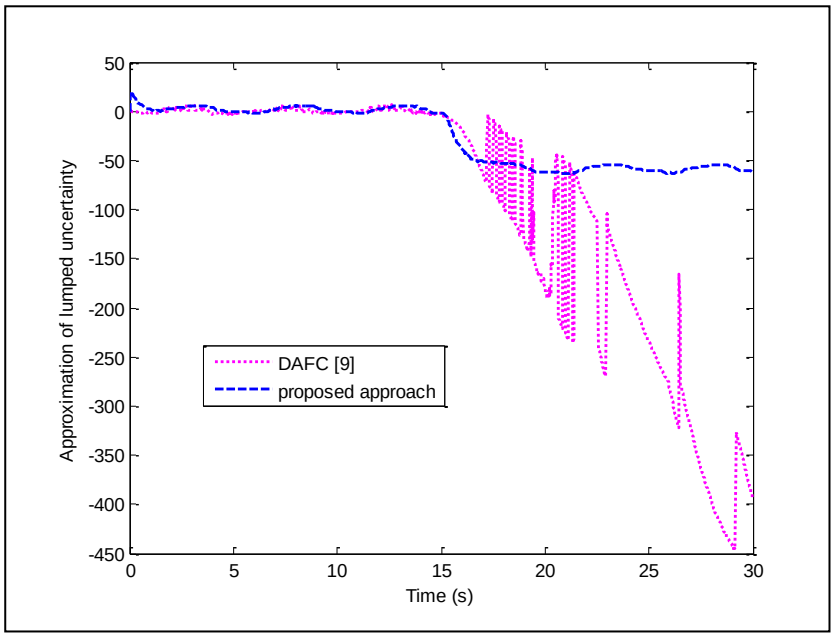

Figure11. Approximation of $\hat{\wp}(t)$

As further work, the experimental results are also measured in terms of several performance indexes quantitatively [15]. The time interval $15 \le t \le 30$ has been selected to compute these indexes in order to avoid transient effects. The results for each one are given in Table 1.

Table1. Performance of four controllers

Index	Unit	DAFC	Proposed Approach
$\max_{15\le t\le 30}\{\lvert e(t)\rvert\}$	(rad)	2.9485	0.4089
$RMS[e(t)]$	(rad)	0.902	0.09653

The first index corresponds to the maximum absolute value of the tracking error defined as $\max_{15\le t\le 30}\{\lvert e(t)\rvert\}$. The best performance for this index was obtained with the proposed control scheme. The improvement for the joint is %86.13concerningthe DAFC controller.

In order to average stochastic effects, the RMS (Root Mean Score) value of the joint position error has also been computed on a trip of time T , that is

$$RMS[e(t)]=\sqrt{\frac{1}{T}\int_0^T \lvert e(\upsilon)\rvert^2 d\upsilon} \tag{61}$$

In practice, the discrete implementation of the criterion Equation (61) leads to

$$RMS[e(t)]=\sqrt{\frac{1}{T}\sum_{\kappa=0}^{i}\lvert e(\kappa h)\rvert^2 h} \quad \text{rad} \tag{62}$$

Where $h=10$ msec is the sampling period, κ is the discrete-time and $T=15\text{sec}$. The best performance index was obtained with the proposed controller because it presented the smallest value of $RMS[e(t)]$, 89.3%, concerning the DAFC controller.

6. Conclusion

This paper presents a robust adaptive control scheme for flexible joint electrically driven robots considering uncertainties in both actuator and manipulator dynamics. The controller design is not dependent on the mechanical dynamics of the actuators and manipulators. Thus, it is free from problems associated with the torque control strategy in the design and implementation. It is shown that the closed-loop system has guaranteed stability while obtains uniformly stability of the joint position error. Experimental results show that tracking performance is satisfactory such that the effects of joint flexibility are well under control. The performance of the control system verifies that the control system is robust against all uncertainties in the manipulator dynamics and its motors. The voltages of motors are permitted under the maximum values.

7. References

[1] Fateh, M. M. 2012. Robust Control of Fexible-Joint Robots using Voltage Control Strategy. Nonlinear Dynamic. 67: 1525-1537.

[2] Sun, C., Gao, H., He, W. and Yu, Y. 2018. Fuzzy Neural Network Control of a Flexible Robotic Manipulator Using Assumed Mode Method. IEEE Transactions on Neural Networks and Learning Systems. 29(11): 5214-5227.

[3] Gao, H., He, W., Zhou, C. and Sun, C. 2018. Neural Network Control of a Two-link Flexible Robotic Manipulator using Assumed Mode Method. IEEE Transactions on Industrial Informatics. 15(2): 755-765.

[4] Qureshi, M. S., Swarnkar, P. and Gupta, S. 2018. A Supervisory Online Tuned Fuzzy Logic based Sliding Mode Control for Robotics: An Application to Surgical Robots. Robotics and Autonomous Systems. 109: 68-85.

[5] He, W., Yan, Z., Sun, Y., Ou, Y. and Sun, C. 2018. Neural-Learning-Based Control for a Constrained Robotic Manipulator with Flexible Joints. IEEE Transactions on Neural Networks and Learning Systems. 29(12): 5993-6003.

[6] Rahmani, B. and Belkheiri, M. 2018. Adaptive Neural Network output Feedback Control for Flexible Multi-link Robotic Manipulators. International Journal of Control. 92(10): 1-15.

[7] Khorashadizadeh, S. and Sadeghijaleh, M. 2018. Adaptive Fuzzy Tracking Control of Robot Manipulators Actuated by Permanent Magnet Synchronous Motors. Computers & Electrical Engineering. 72: 100-111.

[8] Fateh, M. M. 2012. Nonlinear Control of Electrical Flexible-joint Robots. Nonlinear Dynamic. 67: 2549-2559.

[9] Fateh, M.M. 2013. Decentralized Direct Adaptive Fuzzy Control for Flexible-joint Robots. Control Engineering and Applied Informatics. 15(4): 97-105.

[10] Izadbakhsh, A. 2017. FAT-based Robust Adaptive Control of Electrically Driven Robots without Velocity Measurements. Nonlinear Dynamics. 89: 289-304.

[11] Haung, A. C. and Liao, K. K. 2006. FAT-based Adaptive Sliding Control for Flexible Arms: Theory and Experiments. Journal of Sound and Vibration. 298: 194-205.

[12] Huang, A. C., An-chyau, H., Ming-chih, C., and Chien, M. C. 2010. Adaptive Control of Robot Manipulator: A Unified Regressor Free Approach. World Scientific.

[13] Huang, A. C. and Kuo, Y. S. 2001. Sliding Control of Nonlinear Systems Containing Time-Varying Uncertainties with Unknown Bounds. International Journal of Control. 74: 252–264.

[14] Izadbakhsh, A. 2016. Robust Control Design for Rigid-link Flexible-joint Electrically Driven Robot Subjected to Constraint: Theory and Experimental Verification. Nonlinear Dynamic. 85: 751-765.

[15] Moreno-Valenzuela, J., Campa, R. and Santibáñez, V. 2013. Model-based Control of a Class of Voltage-driven Robot Manipulators with Non-passive Dynamics. Computers & Electrical Engineering. 39: 2086-2099.